

**This document was prepared in conjunction with work accomplished under Contract No. DE-AC09-96SR18500 with the U. S. Department of Energy.**

**DISCLAIMER**

**This report was prepared as an account of work sponsored by an agency of the United States Government. Neither the United States Government nor any agency thereof, nor any of their employees, nor any of their contractors, subcontractors or their employees, makes any warranty, express or implied, or assumes any legal liability or responsibility for the accuracy, completeness, or any third party's use or the results of such use of any information, apparatus, product, or process disclosed, or represents that its use would not infringe privately owned rights. Reference herein to any specific commercial product, process, or service by trade name, trademark, manufacturer, or otherwise, does not necessarily constitute or imply its endorsement, recommendation, or favoring by the United States Government or any agency thereof or its contractors or subcontractors. The views and opinions of authors expressed herein do not necessarily state or reflect those of the United States Government or any agency thereof.**

Paper 06421

“CHARACTERISTIC ELECTROCHEMICAL NOISE DURING ELECTROCHEMICAL DETERMINATION OF  
HYDROGEN PERMEATION”

(Karthik H. Subramanian and John I. Mickalonis, Glenn L. Edgemon)

STG 62

Field and Laboratory Advancements in Electrochemical Noise (TEG 099X)

## CHARACTERISTIC ELECTROCHEMICAL NOISE DURING ELECTROCHEMICAL DETERMINATION OF HYDROGEN PERMEATION

Karthik H. Subramanian and John I. Mickalonis  
Westinghouse Savannah River Company  
Savannah River Site  
Aiken SC 29808

Glenn L. Edgemon  
Ares Corp

### ABSTRACT

The Devanathan-Stachurski cell is used to measure hydrogen flux through a metal. The cell consists of galvanostatic cell in which hydrogen is generated on the specimen surface, and an oxidative cell in which the hydrogen oxidation current is measured to determine the hydrogen flux. Permeation has been measured through 304L stainless steel and vanadium alloys. Electrochemical noise analysis has been completed on the potential data collected on the galvanostatic cell specimen surface. The power spectral density using the fast fourier transform and the maximum entropy method have been calculated. The signatures of the power spectral density shown indicate trends in the hydrogen uptake of the materials dependent upon the surface condition including oxide permeability and palladium coating.

Keywords: hydrogen permeation, electrochemical noise

### INTRODUCTION

Hydrogen permeation through a metal involves adsorption, dissociation, solution, diffusion, recombination, and desorption. As such, there are significant surface effects on the hydrogen uptake and permeation through metal alloys. One surface-dependent hydrogen permeation measurement technique is the use of the Devanathan-Stachurski (Devanathan) cell to measure hydrogen uptake, permeation and transport. The Devanathan cell, shown schematically in Figure 1, involves the separation of two independent electrochemical cells with the material of interest. Hydrogen is introduced on one side of the membrane and the hydrogen that permeates is oxidized on the other side. The oxidation current is measured and hydrogen permeability can be calculated, specifically at relatively low temperatures and pressures. The details and permeation results of the testing are given elsewhere, while the analyses of the electrochemical noise on the charging potential are presented herein.<sup>1</sup> The data was analyzed to determine trends in the material-hydrogen interactions and lend insight into surface effects on hydrogen adsorption.

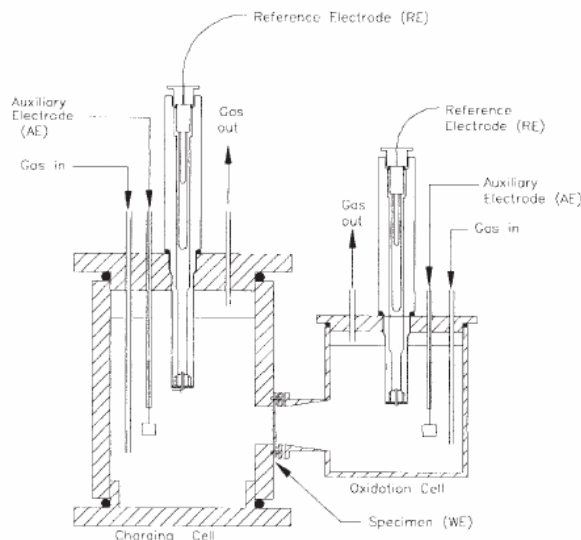


FIGURE 1: Devanathan-Stachurski Cell from ASTM Standard G148

### EXPERIMENTAL

The test matrix consisted of austenitic 304L stainless steel, a vanadium-titanium-nickel alloy, and pure palladium. Some of the samples were plasma deposited with palladium as recommended by ASTM G148. Pure palladium was tested as a reference point. The nominal compositions of the alloys are shown in TABLE 1

TABLE 1: Alloy Composition

| Alloy          | Nominal Alloy Composition (wt%) | X-Ray Mapping (wt%) |
|----------------|---------------------------------|---------------------|
| 304L-SS        | Cr18-Ni12-0.03C <sub>max</sub>  | N/A                 |
| Vanadium Alloy | V51-Ti28-Ni21                   | V72-Ti19-Ni8        |

A brief summary of the experiments is presented, here, while the details are presented elsewhere.<sup>1</sup> The testing was done in 0.1M NaOH solution, at room temperature, utilizing a nitrogen purge before and during measurements. Permeation testing was performed on 304L-SS with and without palladium coating, and vanadium alloys with a palladium coating.

### RESULTS AND DISCUSSION

Interpretation of the electrochemical noise data in such a test is complex because of the surface interactions of the sample as well as the evolution of bubbles. Simple statistical and power spectral density analysis were done on the data sets. The power spectral density for the potential data using the fast fourier transform and the maximum entropy method were calculated.

#### Analysis of Time-Potential Data

The time-potential curves from data measured in the galvanostatic charging side of the Devanathan cell for the alloys are shown in FIGURE 2. The tests were run longer for the pure palladium and vanadium alloys than for the 304L samples. The potential dropped precipitously for the palladium and continued to drop with a lower slope with small noise amplitude. The potential also dropped precipitously for the palladium coated vanadium alloys, but began to rise slightly. The potential noise is large and variable for the stainless steel alloys without a palladium coating, while constant and seemingly cyclical for the palladium coated stainless steel alloy.

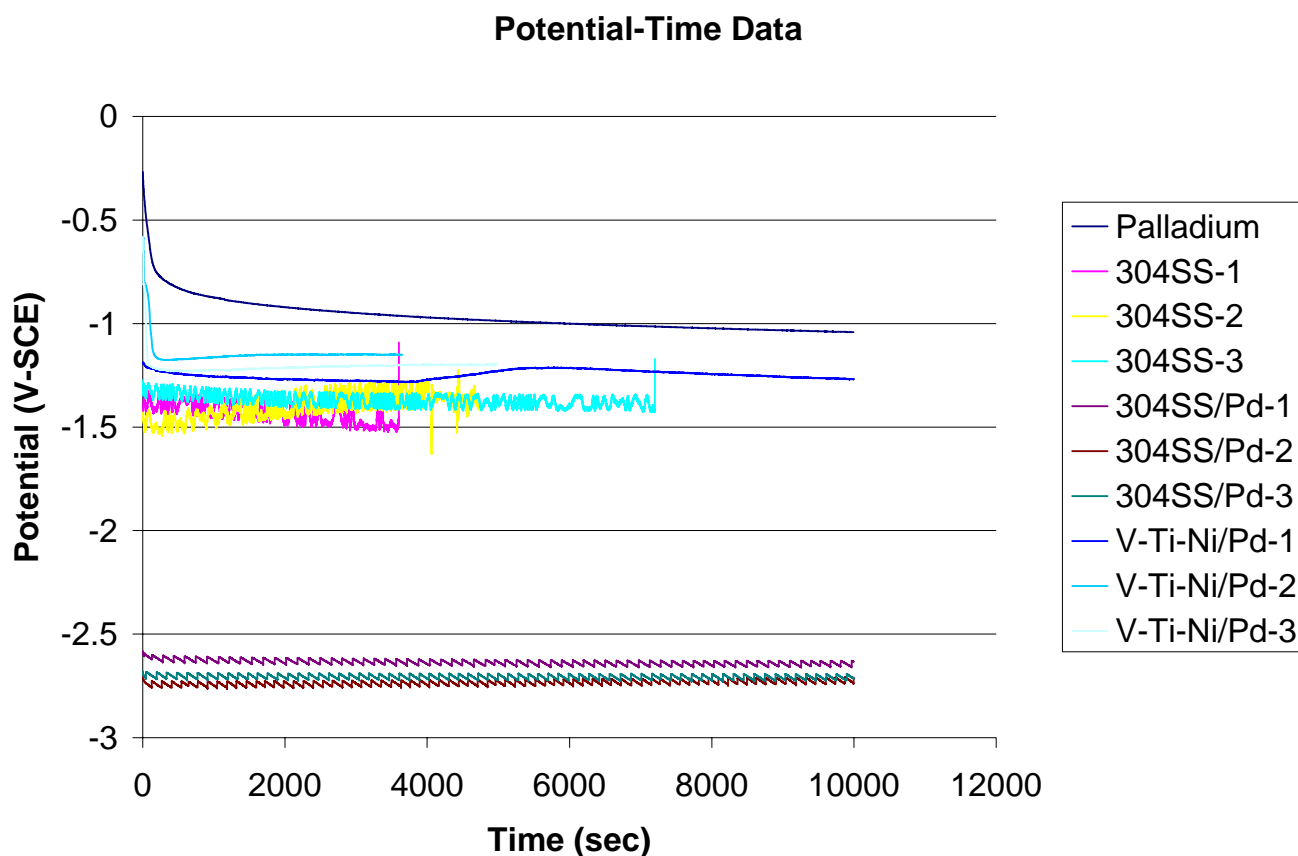


FIGURE 2: Potential-Time Data

The potential fluctuations can be attributed to (1) surface area perturbations due to hydrogen bubble evolution and configuration, and (2) interaction of the hydrogen with the working electrode surface.<sup>2</sup> The adsorption of hydrogen onto and absorption of hydrogen into the surface of the working electrode will also have significant effects on the spectrum. Molecular hydrogen, when it approaches a free surface, can dissociate to form atomic hydrogen. Subsequently, the atomic hydrogen may recombine to form molecular hydrogen or be adsorbed into the metal surface. Similar analysis of charging of low carbon steel showed that the potential noise source could be related to the metal hydrogen interactions at the surface.<sup>3</sup> The noise source was attributed to the presence of the adsorbed hydrogen in the surface layers of the steel surface and the consequent depletion of the hydrogen very near the surface within the solution.

The potential data can be viewed as a combination of the reactions at several interfaces within the working electrode structure, as summarized in FIGURE 3. There are five potential cases of hydrogen-surface-interface interactions:

Case 1: The hydrogen can interact with the oxide surface of a metal as is the case with the stainless steel samples without palladium coatings. The hydrogen must dissociate on the surface of the oxide and penetrate the oxide layer to enter the lattice structure of the underlying metal. The time-potential data in this case shows significant noise, and appears cyclical, which is suspected due to bubble formation and the kinetics of hydrogen permeation through an adherent and relatively permeation resistant oxide layer.

Case 2: The palladium coating remains in intimate contact with the underlying substrate. In this case, the volume expansion does not affect the integrity of the palladium coating onto the metal substrate, thereby allowing atomic hydrogen to permeate from palladium to oxide, without the potential for recombination on the interior palladium interface. The lack of a periodic potential signal typically indicative of bubble formation is also not evident in these curves. The bubble formation on palladium is expected to be minimal, as hydrogen readily dissociates and adsorbs into the palladium structure.

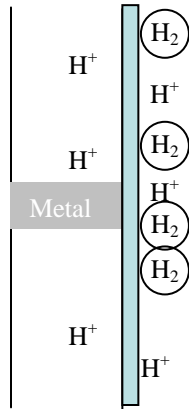
Case 3: A void is created between the palladium coating and the underlying metal oxide (not removed prior to coating) by the volume expansion mismatch of the coating. In this case, hydrogen may recombine at the palladium interface creating bubbles at the metal oxide surface. This interface would now act similar to case 1 where the hydrogen must dissociate on the oxide and penetrate the oxide layer to enter the lattice structure of the underlying metal. The data for the palladium coated stainless steel alloy is representative of this situation. The data is cyclical in nature consistent with Amrani's observations on bubble formation.<sup>2</sup> However, the hydrogen presented at the metal interface in this case is uniform, since the hydrogen presented is a constant function of permeation through the palladium coating and the applied potential.

Case 4: A void is created between the palladium coating and the underlying metal (oxide effectively removed prior to coating) by the volume expansion mismatch of the coating. Once again, in this case hydrogen may recombine and form bubbles at the interface. Once the bubbles form however, the hydrogen absorption is directly into the metal lattice without the permeation barrier of the oxide coating.

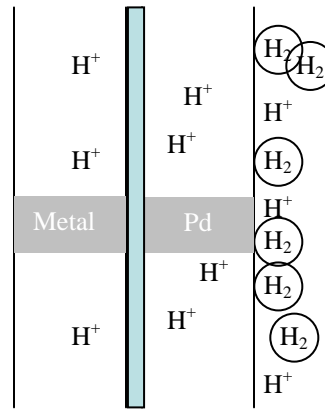
Case 5: An intimate contact between the palladium coating and the pure base metal. This is the ideal case where underlying bubble formation at the metal-Pd interface is prevented and the base metal is free of oxides. This appears to be the case for the data obtained for the palladium coated V-Ti-Ni alloys. In this case, the time potential diagram does not have the nature typical of bubble formation on the surface.

The interaction between the oxides (when present) of the stainless steel ( $\text{Cr}_2\text{O}_3$ ) and the vanadium alloys ( $\text{V}_2\text{O}_5$ , VO) and the hydrogen at the palladium interface may be the controlling mechanism for the hydrogen adsorption. Intermetallic diffusion was considered but unlikely until relatively higher temperature near  $\frac{1}{2}$  the melting point.<sup>4</sup> The oxide layers on stainless steels are known to be thin, and relatively impermeable to hydrogen penetration. For example, the permeability of Type 347 stainless steel was shown to be as much as 400 times lower after exposure to wet hydrogen than clean specimens under identical test conditions.<sup>5</sup> Subsequently, 1000-fold reductions in steady-state permeation rates were found to be introduced by oxidation of Type 446 stainless steels and Fe-20Cr-5Al alloys.<sup>6</sup> Hydrogen is easily adsorbed and rapidly absorbed on clean vanadium surfaces, but surface oxides of the vanadium are known to prevent chemisorption of the hydrogen.<sup>7</sup> Thus, the permeation of the hydrogen through the vanadium alloys is surface limited. The permeation of the hydrogen through the stainless steel is also surface dependent, but the permeation rate through the bulk lattice is relatively slower. Vanadium alloy is a body-centered cubic structure allowing high diffusion of the hydrogen while the face-centered cubic structure of the stainless steel alloys do not allow the high diffusion rates. These data are consistent with lattice structure effects on hydrogen permeation.

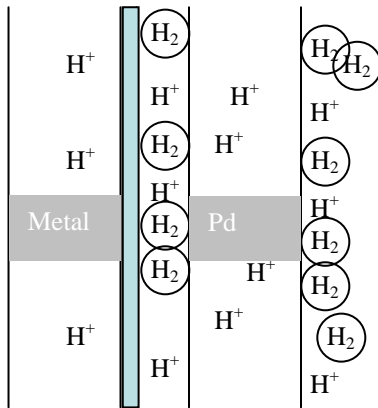
Case 1: Hydrogen interacts with oxide surface of metal



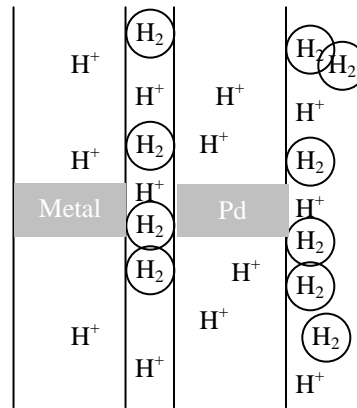
Case 2: Pd coating in intimate contact with oxide interface



Case 3: Pd coating oxide interface is free surface due to volume expansion



Case 4: Pd coating metal interface is free surface due to volume expansion



Case 5: Pd coating is in intimate contact with the metal without oxide

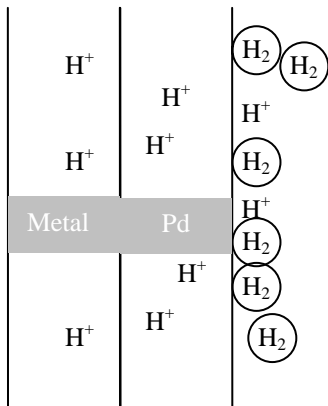


FIGURE 3: Schematic of Possible Interfacial Hydrogen Interactions on Samples

### Statistical Analysis

The statistical analysis including mean, standard deviation, skew, and kurtosis are shown in FIGURE 4. The mean, standard deviation, and the skew are shown on the 1<sup>st</sup> y-axis and the kurtosis is shown on the 2<sup>nd</sup> y-axis due to the large values for the V-Ni-Ti alloy. The statistical analysis did not reveal any broad trends. However, the kurtosis for the vanadium alloys appears to diverge from the other samples.

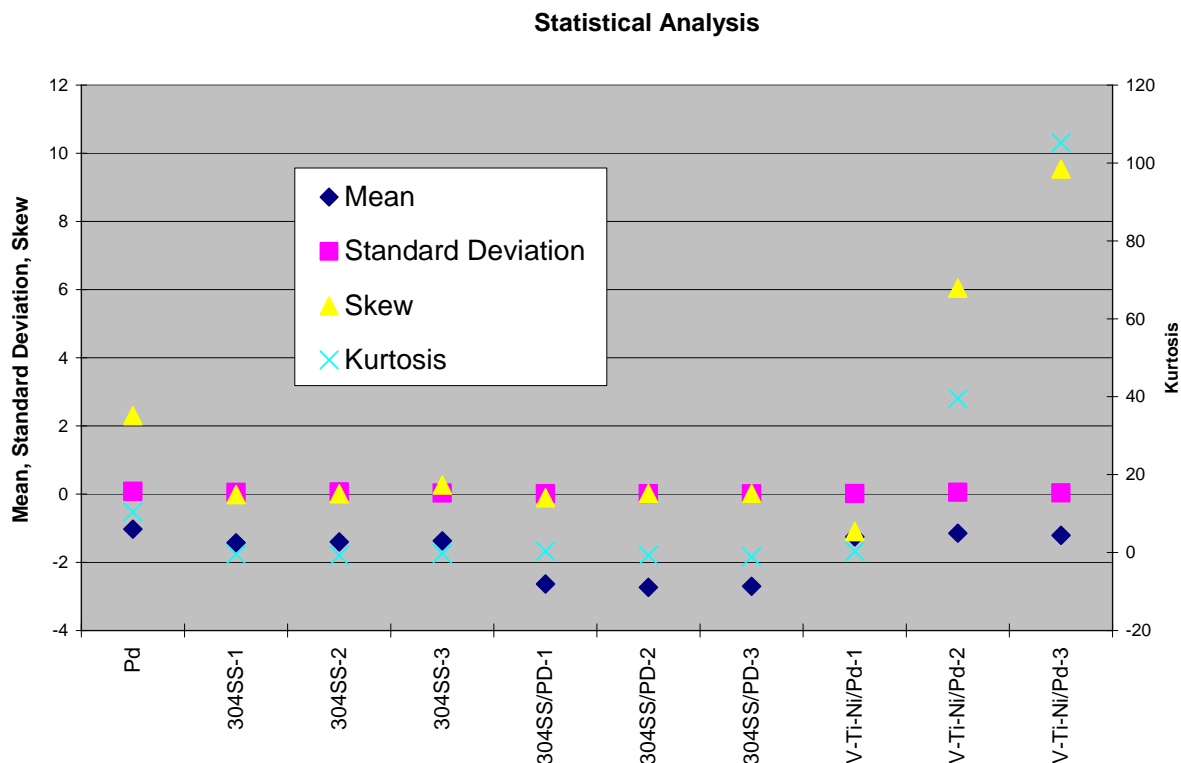


FIGURE 4: Statistical Analysis of Potential Data

### Power Spectral Density Analysis

The power spectral density functions (fast fourier transform and the maximum entropy method) were used to determine electrochemical noise signatures and evaluate trends in the interfacial reactions during permeation testing. The spectra, calculated by the EnAnalyze program, were used to make a comparison between the data obtained.

The fast fourier transforms (FFT) for the data are shown in FIGURE 5 – 7. The FFTs for the alloys of interest are shown with the FFT for palladium for comparison purposes. As expected, the FFT at high frequencies are extremely noisy and don't allow for much interpretation. As such, the maximum entropy method (MEM) was used to calculate the power spectral density.

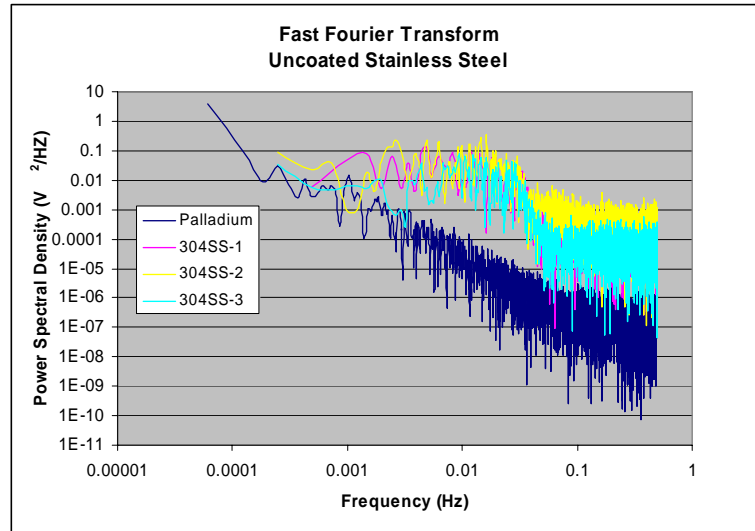


FIGURE 5: Fast Fourier Transform of Charging Potential Data for Uncoated Stainless Steels

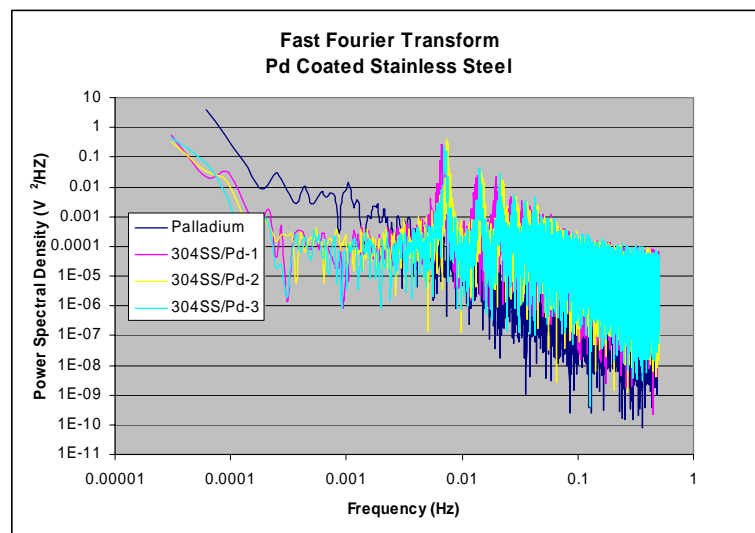


FIGURE 6: Fast Fourier Transform for Charging Potential Data for Pd Coated Stainless Steel.

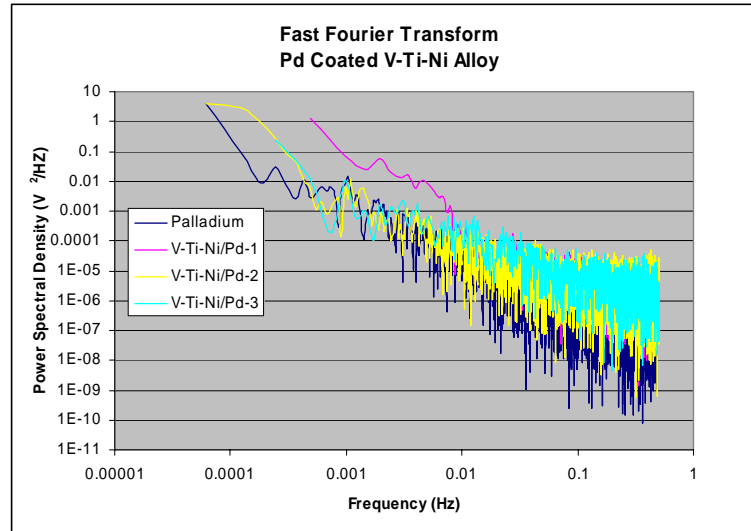


FIGURE 7: Fast Fourier Transform for Charging Potential Data for V-Ti-Ni Alloy

The MEM method was also used to calculate the power spectra. Essentially, the MEM method applies a autocorrelation function (ACF) to the FFT.<sup>8</sup> The MEM data are shown in FIGURE 8. The following trends were observed on the MEM spectra:

- The pure palladium does not change behavior throughout most of the range of frequencies, i.e. until the higher frequencies. This indicates that the hydrogen-palladium interaction appears to be constant and uniform, consistent with the understanding of hydrogen permeation through palladium.
- The V-Ti-Ni samples followed the same behavior as the palladium throughout the range of frequencies. This suggests that the palladium-metal interface is uniform, maintains integrity, and is free of oxides. The influence of oxide thickness (e.g. thin grain boundary oxides) appears masked by the averaging over the surface
- The palladium-coated stainless steels have a plateau region at the lower frequencies while having the same slope as the palladium at the intermediate and higher frequencies. This indicates that there are regions at which the controlling reaction is at the oxide interface, while the hydrogen palladium reactions are represented at those frequencies.
- The uncoated stainless steels have similar behavior in the plateau region and have regions similar to the others at the higher frequencies. However, the behavior, i.e. slope, of the curves varies from the other spectra, possibly suggesting different surface interactions

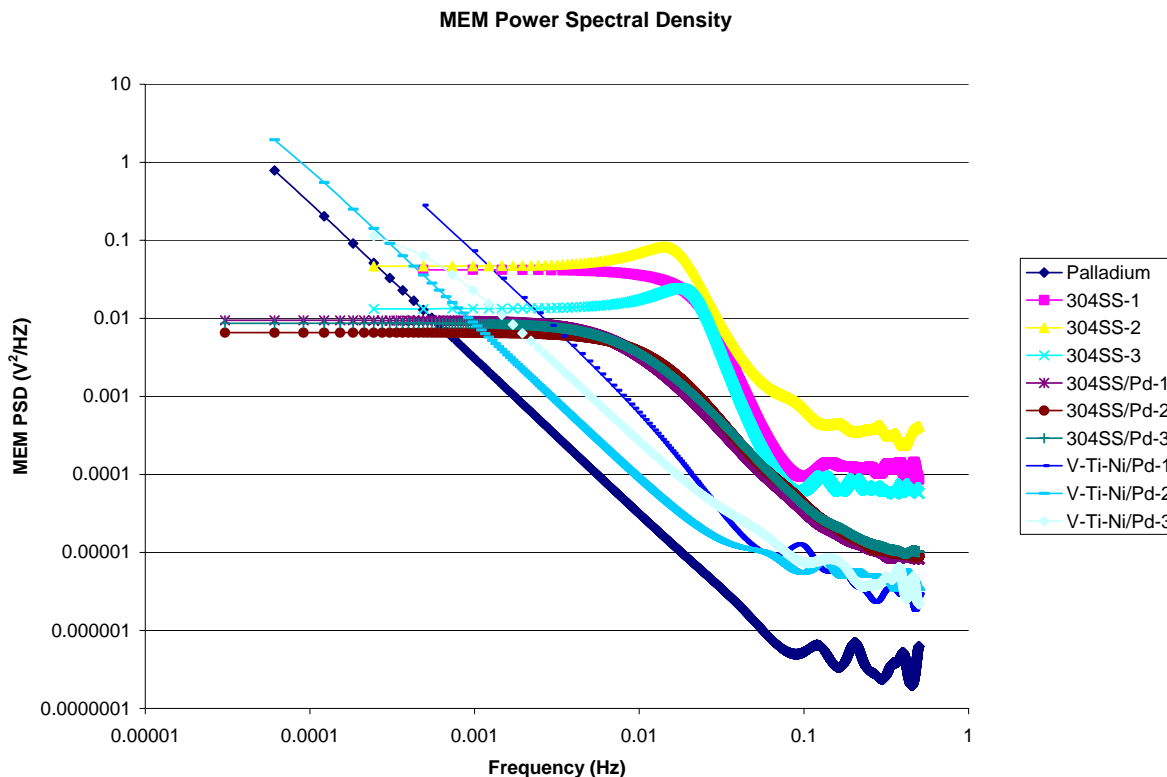


FIGURE 8: MEM Power Spectral Density for the Potential Data

## CONCLUSION

Electrochemical noise analysis of the time-potential data during hydrogen permeation testing utilizing a Devanathan cell reveals metal-hydrogen interactions and can indicate limiting conditions for permeation. The data were analyzed for pure palladium, 304L stainless steel, palladium-coated stainless steels, and palladium coated vanadium-titanium-nickel alloys. The data indicate that careful analysis of the time-potential data and the power spectra can indicate differences in the surface interactions of the hydrogen. In this case, it's clear that the interfacial integrity between palladium coatings and the integrity of the oxide coatings play a key role in the hydrogen adsorption and consequently permeation. The electrochemical noise data analysis can indicate variances in the metal surface-hydrogen interactions, and some signatures have been developed. However, more analysis of the data and testing of additional alloys are planned.

## ACKNOWLEDGMENTS

The author would like to thank Tracy Murphy for technician support in performing the experiments. The authors thank Dr. T. Adams and M. Dupont for technical assistance. This work was performed under Department of Energy (DOE) contract number DE-AC09-96SR18500.

## REFERENCES

1. J. Mickalonis and T. Adams, "Electrochemical Hydrogen Permeation and Oxidation Characteristics of Ni/Ti/Nb Alloys," CORROSION/2006, Paper No. 06437.
2. Z. Amrani, F. Huet, et.al., "Fluctuations of Permeation Rate Through an Iron Membrane Induced by Hydrogen Bubbles," Journal of the Electrochemical Society, **141** (1994) 2059.

3. A. Benzaid and F. Huet, "Electrochemical Noise Analysis of Cathodically Polarised AISI 4140 Steel. II. Identification of Potential Fluctuation Sources for Unstressed Electrodes," *Electrochimica Acta*, **47** (2002) 4325.
4. G.V. Samsanov, *The Oxide Handbook*; IFI/Plenum: New York-Washington-London, 1973.
5. P.S. Flint, USAEC Report KAPL-659 (1951).
6. M.R. Louthan and R.G. Derrick, *Corrosion Science*, **15** (1975) 565.
7. Y. Hatano, et.al. "Permeation of Hydrogen through Vanadium under Helium Ion Irradiation," *Journal of Nuclear Materials*, **283-287- Part 2** (2000) 868.
8. R. A. Cottis, "Interpretation of Electrochemical Noise Data," *Corrosion*, **57 3** (2001) 265.